

# Perturbative calculation of critical exponents for the Bose–Hubbard model

Dennis Hinrichs · Axel Pelster · Martin Holthaus

Published online: 12 April 2013  
© Springer-Verlag Berlin Heidelberg 2013

**Abstract** We develop a strategy for calculating critical exponents for the Mott insulator-to-superfluid transition shown by the Bose–Hubbard model. Our approach is based on the field-theoretic concept of the effective potential, which provides a natural extension of the Landau theory of phase transitions to quantum critical phenomena. The coefficients of the Landau expansion of that effective potential are obtained by high-order perturbation theory. We counteract the divergency of the weak-coupling perturbation series by including the seldom considered Landau coefficient  $a_6$  into our analysis. Our preliminary results indicate that the critical exponents for both the condensate density and the superfluid density, as derived from the two-dimensional Bose–Hubbard model, deviate by less than 1 % from the best known estimates computed so far for the three-dimensional  $XY$  universality class.

## 1 Introduction

The universality of phase transitions is one of the most important concepts in the theoretical description of critical phenomena [1–3]. It implies that continuous phase

transitions fall into universality classes determined by only a few gross properties characterizing the respective system, namely, the number of components of the order parameter and their symmetry, the dimensionality of space, and the range of interaction. Renormalization group (RG) theory then predicts that, e.g., critical exponents are identical for all systems within a given such class. For instance, the lambda transition undergone by liquid  $^4\text{He}$  at the temperature of 2.17 K is the primary example of the three-dimensional  $XY$  universality class, that is, the class with a two-dimensional (or complex) order parameter with  $O(2)$  symmetry in three spatial dimensions, and with short-range interactions. Thus, the critical exponent describing the specific-heat singularity at the lambda point, which was found to be  $\alpha = -0.0127 \pm 0.0003$  in an elaborate zero-gravity experiment [4], should coincide with the corresponding exponent predicted by  $\Phi^4$  theory. Indeed, a seven-loop expansion in three dimensions has resulted in the value  $\alpha = -0.01126 \pm 0.0010$  [5], while  $\alpha = -0.0146 \pm 0.0008$  has been obtained by combining Monte Carlo simulations based on finite-size scaling methods with high-temperature expansions [6]. Evidently, these two theoretical estimates bracket the experimental value, but do not agree with it, nor with themselves, within the margins of uncertainty stated. Thus, this core test of RG theory is not fully conclusive yet; if one accepts the experimental result there still is a need to improve the theoretical calculations.

In this situation, it may be of interest to observe that the notion of universality also includes quantum phase transitions, that is, transitions which occur at zero temperature upon variation of a parameter of the system under consideration, being triggered by quantum rather than thermal fluctuations [7]. In particular, the Mott insulator-to-superfluid transition exhibited by the Bose–Hubbard model on a

---

D. Hinrichs (✉) · M. Holthaus  
Institut für Physik, Carl von Ossietzky Universität,  
26111 Oldenburg, Germany  
e-mail: hinrichs@theorie.physik.uni-oldenburg.de

A. Pelster  
Hanse-Wissenschaftskolleg, Lehmkuhlenbusch 4,  
27753 Delmenhorst, Germany

A. Pelster  
Fachbereich Physik und Forschungszentrum OPTIMAS,  
TU Kaiserslautern, 67663 Kaiserslautern, Germany

$d$ -dimensional cubic lattice falls into the universality class of the  $(d + 1)$ -dimensional  $XY$  model at special multicritical points with particle-hole symmetry [8], implying that the critical exponents provided by the two-dimensional (2D) Bose–Hubbard model should agree with those of the lambda transition. Now that this 2D Bose–Hubbard model has been emulated with ultracold  $^{87}\text{Rb}$  atoms loaded into stacks of planar optical lattices [9, 10], and even the condensate fraction of such a Bose gas in a 2D lattice has been measured across the Mott insulator-to-superfluid transition [11], future precision experiments on this system might enable one to accurately determine the corresponding critical exponents, and thus to provide a further nontrivial test of universality. Indeed, the exploration of critical behavior with ultracold dilute quantum gases has already been taken up by Donner et al. [12], who have measured the critical exponent of the correlation length for a harmonically trapped, weakly interacting 3D Bose gas, albeit with still a comparatively large error bar.

On the theoretical side, the archetypal Bose–Hubbard model lends itself to alternative computational schemes. Only recently, Rançon and Dupuis [13] have presented a detailed RG approach to this model, taking into account both local and long-distance fluctuations. Somewhat alarmingly, the numerical value of the critical exponent for the correlation length of the 2D system derived from that study amounts to  $\nu = 0.699$ , differing quite substantially from the value  $\nu = 0.67155 \pm 0.00027$  previously reported by Campostrini et al. [6]. This finding appears to put universality into question, and hence calls for further independent calculations. In the present paper, we establish a “hands-on” approach to the critical exponents of the Bose–Hubbard model, based on the field-theoretic concept of the effective potential [1, 3], which opens a natural bridge to Landau’s theory of phase transitions [14, 15]. We focus on the exponent  $\beta_c$  for the condensate density, and on the exponent  $\zeta$  for the superfluid density, from which one can deduce all other critical exponents by exploiting (hyper-)scaling relations [16, 17]. We proceed as follows: In Sect. 2 we retrace the basic steps required for deriving the Landau expansion of the effective potential [14, 15], and explain how this expansion is employed for computing both the condensate and superfluid densities. In Sect. 3 we recapitulate the idea of the process chain approach [18], which yields perturbative approximants to the individual Landau coefficients. The results obtained by evaluating the perturbation series numerically to high orders in the hopping strength are then discussed at length in Sect. 4. Here, we encounter a vexing problem, namely, the divergency of weak-coupling perturbation theory. In principle, this calls for a systematic resummation procedure for deducing the “true”, regular Landau coefficients from their diverging polynomial approximants. Nonetheless, here we show that

even *without* such a procedure, but by explicitly including the seldom considered Landau coefficient  $a_6$  into the analysis, one is able to extract critical exponents for the 2D Bose–Hubbard system which agree to better than 1 % with those computed for the lambda transition [6], thus providing fair evidence in favor of universality. Our ad hoc procedure still requires formal justification and hence should be regarded as preliminary, but quite similar results are obtained by applying variational perturbation theory [19]. Some conclusions are drawn in the final Sect. 5.

## 2 The method of the effective potential

The pure Bose–Hubbard model describes Bose particles on a lattice which are allowed to tunnel between neighboring lattice sites, while repelling each other when occupying the same site. In terms of operators  $\hat{b}_i^\dagger$  and  $\hat{b}_i$  which encode the creation and annihilation of a Bose particle at the  $i$ th site and thus obey the commutation relation

$$[\hat{b}_i, \hat{b}_j^\dagger] = \delta_{ij}, \quad (1)$$

it is defined by the grand-canonical Hamiltonian [8]

$$\hat{H}_{\text{BH}} = \hat{H}_0 + \hat{H}_{\text{tun}}, \quad (2)$$

where the site-diagonal part

$$\hat{H}_0 = \frac{1}{2} \sum_i \hat{n}_i(\hat{n}_i - 1) - \mu/U \sum_i \hat{n}_i \quad (3)$$

models the on-site repulsion and fixes the total particle number through the adjustment of the chemical potential  $\mu$ . Here,

$$\hat{n}_i = \hat{b}_i^\dagger \hat{b}_i \quad (4)$$

counts the number of particles at the  $i$ th site and  $U$  is the repulsion energy contributed by any pair of particles sitting on a common site. We are using this energy  $U$  as scale of reference for writing the Hamiltonian in dimensionless form. On the other hand, denoting the energy associated with a hopping event by  $J$ , nearest-neighbor tunneling of the particles is described by

$$\hat{H}_{\text{tun}} = -J/U \sum_{\langle i,j \rangle} \hat{b}_i^\dagger \hat{b}_j, \quad (5)$$

with the angular brackets under the sum indicating that  $i$  and  $j$  are restricted to pairs of adjacent sites. As is well known, the particle-delocalizing tendency of  $\hat{H}_{\text{tun}}$  counteracts the localizing tendency of the repulsive interaction, so that the system exhibits a transition from a Mott insulator to a superfluid when the control parameter  $J/U$  is enhanced gradually, while the scaled chemical potential  $\mu/U$  is kept constant [7, 8].

In order to map out this quantum phase transition, one studies the system’s reaction to the attempt to couple particles into or out of the lattice through spatially homogeneous sources and drains, as expressed by the extended Hamiltonian

$$\widehat{H} = \widehat{H}_{\text{BH}} + \widehat{H}_{\text{s-d}}, \tag{6}$$

where

$$\widehat{H}_{\text{s-d}} = \sum_i (\eta \widehat{b}_i^\dagger + \eta^* \widehat{b}_i). \tag{7}$$

Formally, this step corresponds to explicitly breaking the global particle-number conservation built into  $\widehat{H}_{\text{BH}}$ , the intuitive idea being that the system should resist this attempt for sufficiently small source strength  $\eta$  when being in a Mott insulator state, but show some response for any nonzero  $\eta$  in the superfluid state.

Restricting ourselves to zero temperature, the free energy  $\mathcal{F}$  of the extended system is given by the ground-state expectation value of its Hamiltonian,

$$\mathcal{F}(J/U, \mu/U, \eta, \eta^*) = \langle \widehat{H} \rangle. \tag{8}$$

Assuming the lattice to consist of  $M$  sites (while stipulating that the thermodynamic limit  $M \rightarrow \infty$  be taken eventually), we expand this free energy in the form

$$\mathcal{F}(J/U, \mu/U, \eta, \eta^*) = M \left( f_0(J/U, \mu/U) + \sum_{k=1}^{\infty} c_{2k}(J/U, \mu/U) |\eta|^{2k} \right), \tag{9}$$

so that  $f_0$  denotes the free energy per site of the original system (2). The fact that  $\mathcal{F}$  is expressed here in powers of  $|\eta|^2$ , rather than of  $\eta$  and  $\eta^*$  individually, is understood from the perturbative viewpoint adopted in the following section. If one regards the creation and annihilation operations implementing these sources and drains as individual perturbation events, it is obvious that only processes with an equal number of creation and annihilation events, and hence terms with equal powers of  $\eta$  and  $\eta^*$ , can contribute to the expectation value (8).

Following the guiding insight that the response of the system to the sources or drains, and hence the change of  $\mathcal{F}$  with  $\eta$  or  $\eta^*$ , should reveal its state, it is only natural to consider the intensive quantities

$$\psi = \frac{1}{M} \frac{\partial \mathcal{F}}{\partial \eta^*} = \langle \widehat{b}_i \rangle, \quad \psi^* = \frac{1}{M} \frac{\partial \mathcal{F}}{\partial \eta} = \langle \widehat{b}_i^\dagger \rangle. \tag{10}$$

The respective first equalities in these two relations are nothing but definitions of  $\psi$  and  $\psi^*$ , whereas the respective second equalities follow immediately from the Hellmann–Feynman theorem [20, 21]. Of course, this is the standard way in field theory to introduce the order parameter [1, 3].

The decisive step now is to take  $\psi$  and  $\psi^*$  as new independent variables. This is accomplished by performing a Legendre transformation of  $\mathcal{F}$ , thus constructing the effective potential [14]

$$\Gamma(J/U, \mu/U, \psi, \psi^*) = \mathcal{F} - M(\eta^* \psi + \eta \psi^*), \tag{11}$$

where the old variables  $\eta$  and  $\eta^*$  have to be expressed in terms of  $\psi$  and  $\psi^*$ . To this end, combining the definition (10) with the expansion (9) gives

$$\psi = \eta [c_2 + 2c_4 |\eta|^2 + 3c_6 |\eta|^4 + \mathcal{O}(|\eta|^6)] \tag{12}$$

and its complex conjugate, which then yields

$$\eta = \psi \left[ \frac{1}{c_2} - \frac{2c_4}{c_2^2} |\psi|^2 + \left( \frac{12c_4^2}{c_2^7} - \frac{3c_6}{c_2^6} \right) |\psi|^4 + \mathcal{O}(|\psi|^6) \right] \tag{13}$$

upon inversion. Inserting, one obtains the effective potential (11) as a series in powers of  $|\psi|^2$ :

$$\frac{1}{M} \Gamma = f_0 + a_2 |\psi|^2 + a_4 |\psi|^4 + a_6 |\psi|^6 + \mathcal{O}(|\psi|^8) \tag{14}$$

with coefficients

$$a_2 = -\frac{1}{c_2}, \quad a_4 = \frac{c_4}{c_2^4}, \quad a_6 = \frac{c_6}{c_2^6} - \frac{4c_4^2}{c_2^7}, \tag{15}$$

having suppressed their dependence on  $J/U$  and  $\mu/U$ .

So far, these elementary considerations still refer to the extended system (6), from which the original Bose–Hubbard model (2) is recovered by equating  $\eta = \eta^* = 0$ . By construction,  $\eta$  and  $\psi^*$  on the one hand, and  $\eta^*$  and  $\psi$  on the other, each constitute a Legendre-conjugated pair [22], so that one also has

$$\frac{1}{M} \frac{\partial \Gamma}{\partial \psi^*} = -\eta, \quad \frac{1}{M} \frac{\partial \Gamma}{\partial \psi} = -\eta^*. \tag{16}$$

This is what finally explains why  $\Gamma$  has suggestively been named “effective potential”: setting  $\eta = \eta^* = 0$  in these equations (16) means that the order parameter  $\psi_0$  describing the actual Bose–Hubbard system (2) is determined by finding a stationary point of  $\Gamma$ , in the same manner as a mechanical equilibrium is determined by a stationary point of some given mechanical potential, with stable equilibria corresponding to minima.

Now, we can virtually copy the Landau theory of phase transitions. Assuming  $a_4$  and  $a_6$  to be positive and neglecting higher order terms of the effective potential (14), the minimum of  $\Gamma$  is found at  $\psi_0 = 0$  as long as  $a_2 > 0$ , which indicates the Mott insulator phase. In contrast, when  $a_2 < 0$  the order parameter takes on a nonzero value, signaling the presence of the superfluid phase. Since  $|\psi_0|^2$  then is to be identified with the condensate density  $\varrho_c$ , one has

$$\varrho_c = |\psi_0|^2 = \frac{1}{3a_6} \left( -a_4 + \sqrt{a_4^2 - 3a_2a_6} \right) \quad (17)$$

when  $a_2 < 0$ . Thus, knowledge of solely the coefficient  $a_2(J/U, \mu/U)$  already enables one to locate the phase boundary by means of the condition  $a_2 = 0$  [14]; if one possesses still more information on the effective potential, in the guise of the higher coefficients  $a_4$  and  $a_6$ , say, one can even monitor the appearance of the order parameter when that boundary is crossed, and hence determine the critical exponent  $\beta_c$  of the condensate density.

For computing also the superfluid density  $\varrho_s$  and its critical exponent  $\zeta$ , we recall that if

$$\chi_0(\mathbf{x}) = \exp(i\varphi(\mathbf{x})) |\chi_0(\mathbf{x})| \quad (18)$$

is a single-particle state macroscopically occupied by Bose particles of mass  $m$ , the superfluid velocity  $\mathbf{v}_s(\mathbf{x})$  is defined by the relation [23]

$$\mathbf{v}_s(\mathbf{x}) = \frac{\hbar}{m} \nabla \varphi(\mathbf{x}). \quad (19)$$

Dealing with a  $d$ -dimensional hypercubic lattice, it is convenient to adopt the particular choice

$$\varphi(\mathbf{x}) = \theta \mathbf{e} \cdot \mathbf{x}/L, \quad (20)$$

where  $\mathbf{e}$  is a unit vector in the direction of an arbitrary lattice axis, all of which are equivalent. This means that the phase progresses by the twist angle  $\theta$  on each path of length  $L$  parallel to  $\mathbf{e}$ . The twist is imposed on the many-body wave function  $\Psi$  by requiring [24, 25]

$$\Psi(\dots, \mathbf{x}_j + L\mathbf{e}, \dots) = e^{i\theta} \Psi(\dots, \mathbf{x}_j, \dots) \quad (21)$$

for each particle (labeled here by  $j$ ). Operationally, this is achieved by performing the local unitary transformation

$$\hat{b}_i \rightarrow e^{i\varphi(\mathbf{x}_i)} \hat{b}_i, \quad \hat{b}_i^\dagger \rightarrow e^{-i\varphi(\mathbf{x}_i)} \hat{b}_i^\dagger, \quad (22)$$

where  $\mathbf{x}_i$  is the position of the lattice site No.  $i$ ; in this way, the boundary conditions are shifted onto the Hamiltonian. Now let  $\mathcal{F}(\theta)$  be the free energy (8) as belonging to the “twisted” Hamiltonian which gives rise to superfluid flow, denote the number of lattice sites inside the hypercube  $L^d$  by  $M$ , and specify  $\varrho_s$  as the number of superfluid particles per lattice site. If the particles were free, this would imply

$$\begin{aligned} U[\mathcal{F}(\theta) - \mathcal{F}(0)] &= M\varrho_s \frac{m}{2} \mathbf{v}_s^2 \\ &= M\varrho_s \frac{m}{2} \left( \frac{\hbar}{m} \right)^2 \left( \frac{\theta}{L} \right)^2. \end{aligned} \quad (23)$$

But since the single-particle dispersion relation actually reads

$$E(\mathbf{k}) = -2J \sum_{j=1}^d \cos(k_j a), \quad (24)$$

where  $a$  is the lattice constant, one has to replace the factor  $\hbar^2/(2m)$  in Eq. (23) by  $Ja^2$ . Moreover, by virtue of the geometrical properties of the Legendre transformation [22] the free energy equals the effective potential when the latter is evaluated at its minimum  $\psi_0$  [15]. Taken together, this gives

$$U[\Gamma(\theta)|_{\psi_0} - \Gamma(0)|_{\psi_0}] = M\varrho_s Ja^2 \left( \frac{\theta}{L} \right)^2 \quad (25)$$

for sufficiently small  $\theta/L$ . Measuring lengths in multiples of the lattice constant and hence writing  $\ell = L/a$ , this finally leads to

$$\varrho_s = \lim_{\theta \rightarrow 0} \frac{1}{MJ/U} \left( \frac{\ell}{\theta} \right)^2 [\Gamma(\theta)|_{\psi_0} - \Gamma(0)|_{\psi_0}]. \quad (26)$$

This expression is closely related to the helicity modulus introduced by Fisher et al. [16], emphasizing that the superfluid density quantifies the rigidity of the system under the imposed twist. Thus, sufficient knowledge of the effective potential, both with and without such a twist, enables one to monitor the emergence of  $\varrho_s$  when the phase boundary is crossed upon varying  $J/U$ , and thereby to determine its critical exponent  $\zeta$ .

### 3 The process-chain approach to compute the effective potential

The main computational task now consists in the calculation of the expansion coefficients  $a_{2k}$  of the effective potential (14), which, according to Eq. (15), are given in terms of the coefficients  $c_{2k}$  introduced in the expansion (9) of the free energy, either without or including an additional phase twist (22). We obtain these coefficients by means of the process-chain approach devised by Eckardt [18], which is based on a formulation of the perturbation series going back to the Japanese mathematician Tosio Kato [26, 27]: consider a Hamiltonian  $\hat{H}_0$  with a nondegenerate eigenstate  $|m\rangle$  and corresponding eigenvalue  $E_m^{(0)}$  which is subjected to some suitable perturbation  $\hat{V}$ , such that the total Hamiltonian becomes  $\hat{H} = \hat{H}_0 + \hat{V}$ . Then the  $n$ th-order contribution  $E_m^{(n)}$  to the perturbation series

$$E_m = E_m^{(0)} + \sum_{n=1}^{\infty} E_m^{(n)} \quad (27)$$

for the eigenvalue  $E_m$  of  $\hat{H}$  which evolves from  $E_m^{(0)}$  upon turning on the perturbation can be written in the nonrecursive form [26, 27]

$$E_m^{(n)} = \text{tr} \left[ \sum_{\mathcal{A}_n} \hat{S}^{\alpha_1} \hat{V} \hat{S}^{\alpha_2} \hat{V} \hat{S}^{\alpha_3} \dots \hat{S}^{\alpha_n} \hat{V} \hat{S}^{\alpha_{n+1}} \right], \quad (28)$$

where the chain operators  $\widehat{S}^\alpha$  concatenating the  $n$  perturbing operators  $\widehat{V}$  are given by

$$\widehat{S}^\alpha = \begin{cases} -|m\rangle\langle m| & \text{for } \alpha = 0 \\ \sum_{i \neq m} \frac{|i\rangle\langle i|}{(E_m^{(0)} - E_i^{(0)})^\alpha} & \text{for } \alpha > 0, \end{cases} \quad (29)$$

and the sum extends over all sets of  $n + 1$  nonnegative integers  $\alpha_j$  which sum up to  $n - 1$ ,

$$\Lambda_n = \left\{ (\alpha_1, \dots, \alpha_{n+1}) \mid \sum_{j=1}^{n+1} \alpha_j = n - 1 \right\}. \quad (30)$$

By means of standard manipulations [18, 28], the individual terms arising from Kato’s trace formula (28) can be cast into matrix elements of the form

$$\langle m | \widehat{V} \widehat{S}^{\alpha_1} \widehat{V} \widehat{S}^{\alpha_2} \dots \widehat{S}^{\alpha_{n-1}} \widehat{V} | m \rangle, \quad (31)$$

to be multiplied with certain weight factors. These matrix elements allow for an intuitive interpretation: starting from the initial state  $|m\rangle$ , the system undergoes a chain of  $n$  subsequent perturbation processes before finally returning to  $|m\rangle$ . If there are no selection rules making some of these matrix elements vanish, their number increases by a factor of more than 2 when advancing from  $n$  to  $n + 1$ : one faces ten elements in 5th order, but already 627 for  $n = 10$  [18, 28].

In our case, the “unperturbed” operator  $\widehat{H}_0$  is given by the site-diagonal component (3) of the Bose–Hubbard Hamiltonian, the eigenstates of which are characterized by sharp occupation numbers for each lattice site. We consider a Mott state with integer filling factor  $g$ , that is, a state with  $g$  particles residing on each site:

$$|m\rangle = \prod_i \frac{(\widehat{b}_i^\dagger)^g}{\sqrt{g!}} |0\rangle, \quad (32)$$

where  $|0\rangle$  is the empty-lattice state. In what follows we restrict ourselves to  $g = 1$ , meaning that we have to adjust  $\mu/U$  accordingly. The perturbation is given by the tunneling Hamiltonian (5) combined with the sources and drains described by the symmetry-breaking extension (7), so that

$$\widehat{V} = \widehat{H}_{\text{tun}} + \widehat{H}_{\text{s-d}}, \quad (33)$$

and the goal is to evaluate the perturbation series (27) for  $\langle \widehat{H} \rangle = E_m$ . Now the representation (9) tells us that the desired quantities  $c_{2k}$  emerge as prefactors of  $|\eta|^{2k}$  in a series expansion of  $E_m/M$  with respect to powers of  $|\eta|^2$ , and therefore are given by all process chains containing  $k$  creation operators  $\widehat{b}_i^\dagger$  and further  $k$  annihilation operators  $\widehat{b}_j$ . Hence, when considering a formal hopping expansion of these functions,

$$c_{2k} = \sum_{v=0}^{\infty} \gamma_{2k}^{(v)} (J/U)^v, \quad (34)$$

$n$ th-order perturbation theory gives access to the coefficients  $\gamma_{2k}^{(v)}$  with  $v = n - 2k$ , assuming  $n \geq 2k$ . By construction, these coefficients embody the collection of all process chains with  $k$  creation and  $k$  annihilation events, and  $n - 2k$  additional hopping events; a diagrammatic representation of the lowest-order contributions to  $c_2$ ,  $c_4$ , and  $c_6$  is depicted in Fig. 1. When mastering this process-chain approach in higher orders, the computational bottleneck does not lie in the determination of the comparatively few Kato terms (31), but rather in the fact that for each such term one has to consider all permutations of the respective processes [28]—requiring us to deal with  $12! = 479,001,600$  permutations for  $n = 12$ , which is the maximum order considered in the present paper.

Nonetheless, this process-chain approach can be implemented in a numerically efficient manner. So far, we have employed this technique for computing accurate phase boundaries for cubic lattices with arbitrary filling factors [28, 29], for establishing a scaling property of the critical hopping strengths [30], and for determining the critical parameters for both triangular and hexagonal lattices [31]. In a more recent study of Bose–Hubbard and Jaynes–Cummings lattice models, the process-chain approach has been judged to be extremely powerful [32]; a closely related scheme has been utilized successfully for evaluating high-order terms for the fermionic Hubbard model [33]. In the following chapter, we will report our preliminary results obtained when applying the perturbative process-chain approach for the determination of the effective potential of the Bose–Hubbard model, and, in a straightforward further step, for the calculation of critical exponents.

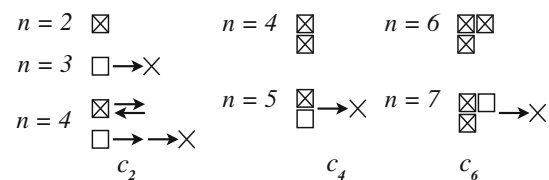


**Fig. 1** Diagrammatic representation of the lowest-order contributions to the quantities  $c_2$ ,  $c_4$ , and  $c_6$ . Creation and annihilation processes are symbolized by *open boxes* and *crosses*, respectively; each *arrow* denotes a tunneling process between neighboring lattice sites. In general, the coefficients  $\gamma_{2k}^{(v)}$  introduced in the formal expansion (34) incorporate all chains with  $k$  creation events,  $k$  annihilation events, and  $v = n - 2k$  tunneling events. The determination of all such diagrams, and their respective weights, is accomplished by the process-chain approach

## 4 Results

Having gone through the preceding deliberations, the roadmap now is plainly laid out. The process-chain approach is employed for computing polynomial approximations to the coefficients  $c_{2k}(J/U, \mu/U)$ . These are rearranged to provide corresponding approximations to the coefficients  $a_{2k}(J/U, \mu/U)$  appearing in the Landau expansion (14) of the effective potential, from which one then

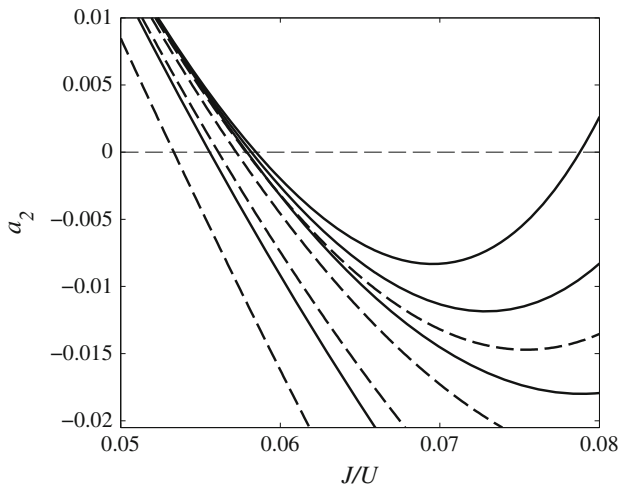


**Fig. 2** Successive perturbational approximants to the Landau coefficient  $a_2$  for the 2D Bose–Hubbard model with scaled chemical potential  $(\mu/U)_c = 0.373$ , as corresponding to the tip of the Mott lobe with filling factor  $g = 1$ . Starting with the *leftmost* line, and proceeding counter-clockwise, the respective maximum hopping orders  $v_m$  are 3, 2, 5, 7, 4, 9, 6, and 8. Here and in the following Figs. 5–7, *full lines* refer to even and *dashed lines* to odd  $v_m$

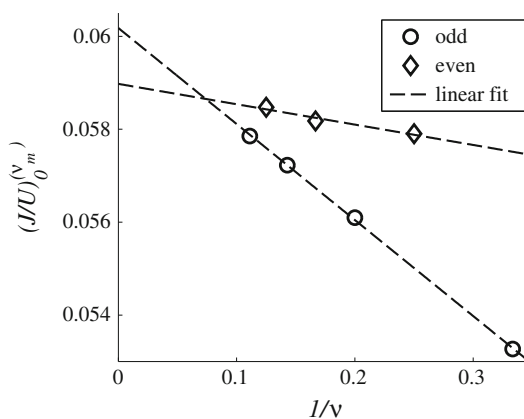


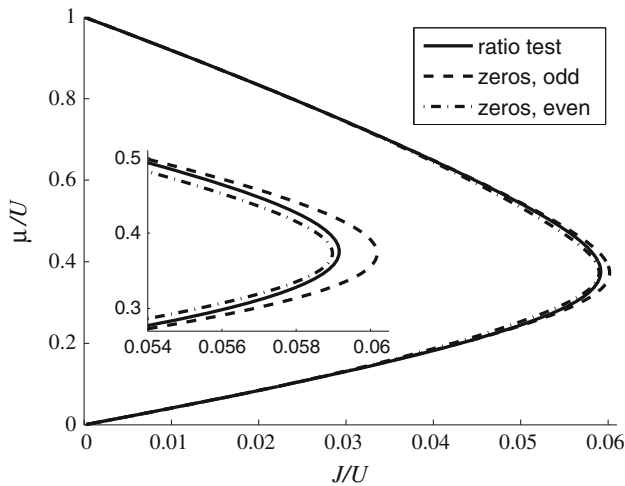
**Fig. 3** Zeros  $(J/U)_0^{(v_m)}$  of the approximants to  $a_2$  shown in Fig. 2, plotted versus the inverse maximum hopping order. Observe that *data points* belonging to odd or even  $v_m$  can be fitted separately to *straight lines*. The extrapolations of these lines to the *left margin* provide upper and lower bounds on the critical-scaled hopping strength  $(J/U)_c$

obtains the condensate density  $\rho_c$  and, after inclusion of a phase twist, the superfluid density  $\rho_s$ .

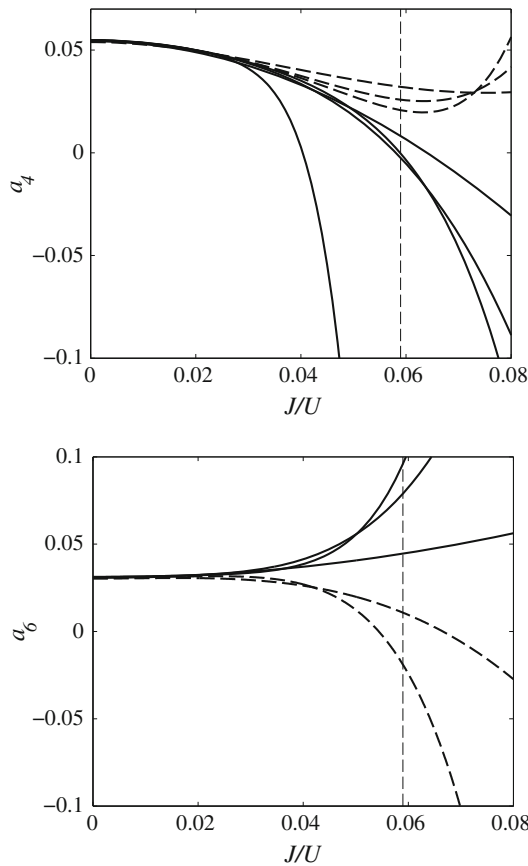
Figure 2 shows results for the coefficient  $a_2$  for the 2D Bose–Hubbard model with fixed chemical potential  $(\mu/U)_c = 0.373$ , as corresponding to the border between the Mott insulator and the superfluid state with filling factor  $g = 1$  (see also Fig. 4 below). Maximum hopping orders taken into account here range from  $v_m = 2$  to  $v_m = 9$ , matching the orders  $n = 4$  to  $n = 11$  of the perturbation series. The zeros of the successive approximants to  $a_2$ , considered as functions of the scaled hopping strength  $J/U$ , mark the respective estimates  $(J/U)_0^{(v_m)}$  of the scaled critical hopping strength  $(J/U)_c$  for  $g = 1$ ; these zeros are plotted in Fig. 3 over the inverse hopping order. Evidently, data points resulting from odd and even  $v_m$  can separately be fitted to straight lines; the extrapolations of these lines for  $v_m \rightarrow \infty$ , or  $1/v_m \rightarrow 0$ , should contain information on the true value of  $(J/U)_c$ . Alternatively one can compute the phase boundary by means of the “ratio-test” method, which amounts to estimating the apparent radius of convergence of the series (34) for  $c_2$  [28, 29], instead of determining the zero of  $a_2 = -1/c_2$ . Including contributions up to  $n = 11$ , we find  $(J/U)_c \approx 0.05920$  in this manner, suggesting that the two extrapolated values inferred from Fig. 3 serve as upper and lower bounds on the actual value. If one accepts this hypothesis, the possible error of our phase boundary is at most on the order of 2 %. Indeed, this estimate is well compatible with the result  $(J/U)_c = 0.05974(3)$  provided by quantum Monte Carlo (QMC) simulations [34].

Figure 4 then depicts the entire lowest Mott lobe for the 2D Bose–Hubbard model, i.e., the boundary between the Mott insulator state with  $g = 1$  (inside the lobe) and the superfluid state (outside); here, the result provided by the ratio test is framed by the two bounds determined according to the scheme depicted in Fig. 3. In order to compute the critical exponents of the quantum phase transition, we have to focus on the tip of this lobe [8].

Perturbative approximants to the higher effective potential coefficients  $a_4$  and  $a_6$  for the 2D Bose–Hubbard model are displayed in Fig. 5; note that the computation of  $a_4$  with  $v_m = 8$ , or that of  $a_6$  with  $v_m = 6$ , necessitates to evaluate the perturbation series even to 12th order. In marked contrast to  $a_2$ , now the successive “approximations” do not approach each other with increasing  $v_m$  in the vicinity of  $(J/U)_c$ , but rather appear to diverge strongly in an alternating manner; increasing accuracy with increasing  $v_m$  is achieved only for comparatively small  $J/U$ . Evidently we are dealing with asymptotic series; to deduce the true behavior of both  $a_4$  and  $a_6$  close to the phase transition, one needs to convert the divergent weak-coupling series into convergent strong-coupling expansions. Techniques for



**Fig. 4** Mott lobe with filling factor  $g = 1$  for the 2D Bose–Hubbard model, computed with the “ratio-test” method put forward in Refs. [28, 29]. Also shown are the bounds obtained by the procedure sketched in Fig. 3



**Fig. 5** Upper panel approximants to the coefficient  $a_4$  for  $d = 2$  and  $(\mu U)_c = 0.373$ , as in Fig. 2. Starting with the leftmost line crossing the lower margin, and proceeding counter-clockwise along the margin, the respective maximum hopping orders  $v_m$  are 8, 6, 4, 2, 3, 5, 7. Lower panel approximants to the coefficient  $a_6$  for  $d = 2$  and  $(\mu U)_c = 0.373$ . Starting with the line crossing the lower margin and proceeding counter-clockwise, the respective maximum hopping orders  $v_m$  are 5, 3, 2, 4, 6. Vertical dashed lines mark  $(J/U)_c$

doing this do exist [35], but would require some a priori information on the functional form of the true  $a_4$  and  $a_6$ . A similar pattern is also observed in Fig. 6, in which corresponding plots of  $a_2$ ,  $a_4$ , and  $a_6$  for the 3D system with  $g = 1$  are grouped together. While successive estimates of the zero of  $a_2$  actually come closer to each other with increasing  $v_m$ , allowing one to determine  $(J/U)_c \approx 0.03407$  by extrapolation, successive approximants to  $a_4$  and  $a_6$  repel each other in the vicinity of  $(J/U)_c$ , although this divergence appears to be somewhat less violent here than for  $d = 2$ . Again, our above estimate of  $(J/U)_c$  compares very favorably with the QMC result  $(U/J)_c = 29.34(2)$  [36].

However, we are not primarily interested in the individual Landau coefficients (15), but rather in the full effective potential (14). It is, therefore, interesting to observe that the divergent behavior of the perturbative approximants to  $a_6$  appears to counteract the divergency of the approximants to  $a_4$ : whereas the odd-order approximants (dashed lines) appear to “overshoot” the true values of  $a_4$  for both the 2D (Fig. 5) and 3D systems (Fig. 6), they tend to “undershoot” the respective true values of  $a_6$ , and vice versa for the even orders (full lines). Moreover, these higher coefficients enter into  $\Gamma$  only to higher orders in  $|\psi|^2$ , while we require accurate knowledge of  $\Gamma$  for small  $|\psi|$ . Thus, there is some hope that one still obtains a useful approximation to the effective potential even from the nonresummed coefficients. This hypothesis is supported by Fig. 7, which depicts successive approximants to the effective potential  $\Gamma/M$  for the 2D system, as computed from  $a_2$ ,  $a_4$ , and  $a_6$  as functions of  $|\psi|$ . The upper panel refers to  $J/U = 0.055$ ; the trend of the graphs with increasing  $v_m$  suggests that the higher-order approximants indeed yield an acceptable estimate of  $\Gamma$  in the full range  $0 \leq |\psi| \leq 0.1$  considered. The lower panel shows a similar plot for  $J/U = 0.059$ , quite close to the critical value, where one still finds a fairly reasonable behavior of the approximants even up to  $|\psi| = 0.5$ .

This observation allows us to proceed, albeit tentatively, with the perturbative approximants to the coefficients (15), and to use these for computing the condensate density  $\varrho_c$  by means of Eq. (17). Here we admit even-order approximants only, since according to Figs. 5 and 6 only even  $v_m$  provide positive  $a_6$ , and hence guarantee a stable, confining effective potential when terminating the Landau expansion (14) after the sixth-order term; approximants with odd  $v_m$  are disregarded. Moreover, when Eq. (26) is evaluated likewise with a sufficiently small value of the twist  $\theta/\ell$ , it yields a corresponding estimate of the superfluid density  $\varrho_s$ . Figure 8 shows results thus obtained with  $v_m = 6$  for  $d = 2$  (main frame), and with  $v_m = 4$  for  $d = 3$  (inset). Both densities initially increase about linearly for  $d = 3$ , heralding trivial (mean-field) critical exponents  $\beta_c = 1$  for  $\varrho_c$ ,

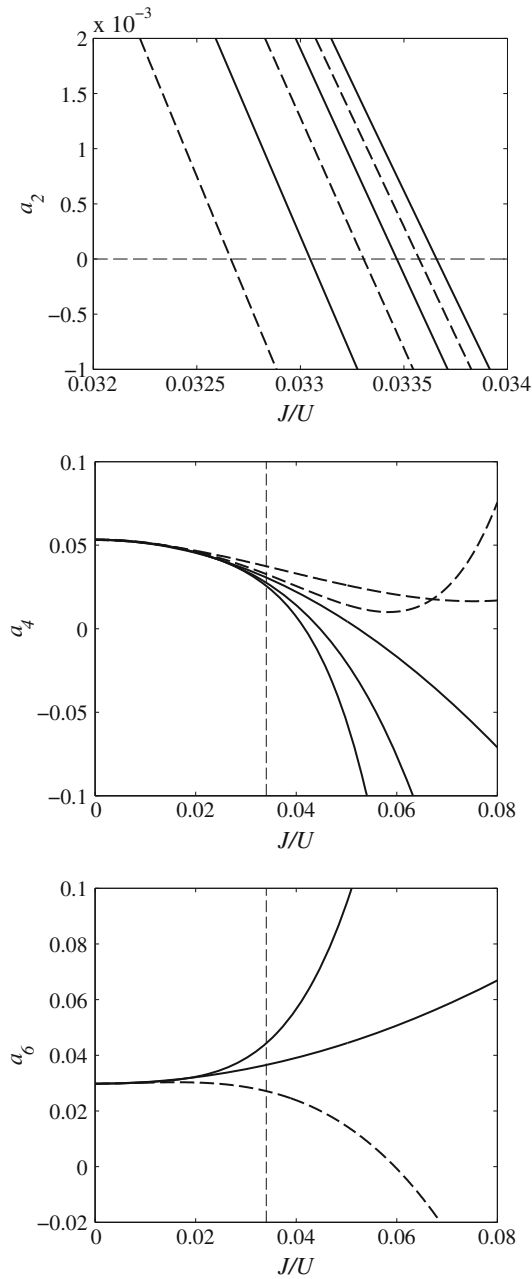


**Fig. 6** Upper panel successive perturbational approximants to the Landau coefficient  $a_2$  for the 3D Bose–Hubbard model with scaled chemical potential  $(\mu/U)_c = 0.393$ , as corresponding to the tip of the Mott lobe with filling factor  $g = 1$ . Starting with the leftmost straight line and proceeding rightwards, the respective maximum hopping orders  $\nu_m$  are 3, 2, 5, 4, 7, 6. Middle panel as above for the coefficient  $a_4$ . Starting with the leftmost line crossing the lower margin, and proceeding counter-clockwise along the margin, maximum hopping orders  $\nu_m$  are 6, 4, 2, 3, 5. Lower panel as above for the coefficient  $a_6$ . Maximum hopping orders  $\nu_m$ , assigned as above, are 3, 2, 4. Vertical dashed lines mark  $(J/U)_c$

and  $\zeta = 1$  for  $q_s$ . This is to be expected, because the 3D Bose–Hubbard system belongs to the universality class of the 4D XY model; since  $d = 4$  is the upper critical

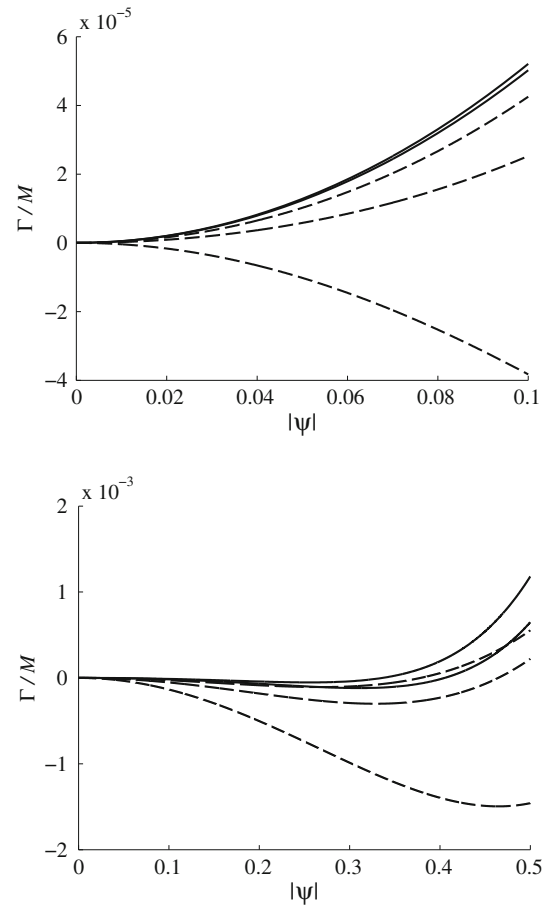


**Fig. 7** Effective potential  $\Gamma(\psi)/M$  evaluated for the 2D Bose–Hubbard model with  $(\mu/U)_c = 0.373$ , and  $J/U = 0.055$  (above) or  $J/U = 0.059$  (below). Proceeding from bottom to top at the right margin, maximum hopping orders  $\nu_m$  are 3, 5, 7, 4, 6 for both panels

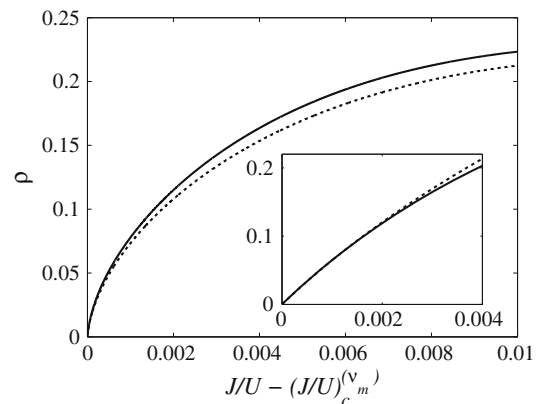


**Fig. 8** Superfluid density  $q_s$  (full lines) and condensate density  $q_c$  (dotted) for  $d = 2$  with  $\nu_m = 6$  (main frame), and for  $d = 3$  with  $\nu_m = 4$  (inset). While the close-to-linear increase of both densities for  $d = 3$  yields the expected mean-field exponents  $\beta_c = \zeta = 1$ , one finds nontrivial exponents for  $d = 2$ . The superfluid densities have been computed with the twist  $\theta\ell = 0.001$

dimension of this latter model, mean-field theory provides the correct critical exponents for this dimension, and all higher ones. On the other hand, the 2D Bose–Hubbard system falls into the 3D XY universality class; in this case the exponents are nontrivial. Thus, although the Bose–Hubbard system with  $d = 3$  spatial dimensions is computationally more demanding,  $d = 2$  is the case of main interest. Indeed, Fig. 8 clearly indicates that the exponents for  $d = 2$  must be significantly lower than 1; from the fact that the 2D condensate density  $\rho_c$  (dotted) lies below the superfluid density  $\rho_s$  (full line) one deduces that the exponent  $\beta_c$  of  $\rho_c$  is larger than the exponent  $\zeta$  of  $\rho_s$ . This finding is in line with the Josephson relation [16, 17, 37]

$$\zeta = \beta_c - \eta\nu, \tag{35}$$

where  $\nu$  is the critical exponent of the correlation length, as already referred to in the “Introduction” section, and  $\eta$  is the critical exponent of the correlation function.

Assuming now that the densities behave as

$$\rho \propto (J/U - (J/U)_c)^x \tag{36}$$

for  $J/U$  somewhat larger than  $(J/U)_c$ , the respective critical exponent  $x$  is unveiled by computing the logarithmic derivative

$$D \log \rho = \frac{d \log \rho}{d \log (J/U - (J/U)_c)} \tag{37}$$

and taking the limit

$$x = \lim_{J/U - (J/U)_c \rightarrow 0} D \log \rho. \tag{38}$$

In Fig. 9 we plot the logarithmic derivative (37) of  $\rho_c$  for both  $d = 2$  as obtained from approximations with either  $\nu_m = 4$  or  $\nu_m = 6$ , and for  $d = 3$  with  $\nu_m = 4$ . Evidently, these derivatives behave almost linearly over wide ranges

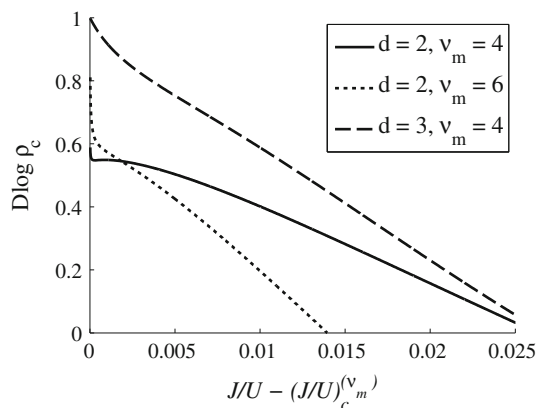


**Fig. 9** Logarithmic derivative (37) of the condensate density  $\rho_c$ , computed according to Eq. (17) for  $d = 2$  with both  $\nu_m = 4$  and  $\nu_m = 6$ , and for  $d = 3$  with  $\nu_m = 4$ . Observe that continuing the linear part of the graph for  $d = 3$  to  $J/U - (J/U)_c = 0$  yields  $\beta_c = 1$  with reasonable accuracy, whereas the data for  $d = 2$  clearly suggest a smaller value

**Table 1** Finite-order estimates of the critical exponent  $\beta_c$  for the condensate density  $\rho_c$ , and of the critical exponent  $\zeta$  for the superfluid density  $\rho_s$ , as obtained for the 2D Bose–Hubbard model

$\nu_m \setminus \theta/\ell$	$\beta_c^{(\nu_m)}$	$\zeta^{(\nu_m)}$	
		0.001	0.01
4	0.5715	0.6446	0.6463
6	0.6153	0.6525	0.6541
$\infty$	0.7029	0.6683	0.6697
$\theta/\ell \rightarrow 0$	–	0.6681	

Also listed are their extrapolations to infinite order, performed linearly in  $1/\nu_m$ . In the case of  $\zeta$  two values of the twist  $\theta/\ell$  are considered, providing data which are extrapolated separately to  $\nu_m = \infty$ ; a further linear extrapolation then yields the desired limit for  $\theta/\ell \rightarrow 0$

of  $J/U$ , with the exception of the immediate vicinity of  $(J/U)_c$ . But this latter regime has to be ignored anyway, because all our numerical results are given in terms of power series, thus isolating a single term close to  $(J/U)_c$ , whereas several powers have to combine in order to mimic noninteger exponents. Therefore, we obtain plausible finite-order estimates  $\beta_c^{(\nu_m)}$  of the condensate-density exponent  $\beta_c$  by extending the linear slopes to  $J/U - (J/U)_c = 0$ . To begin with, for  $d = 3$  we have  $\beta_c^{(4)} \approx 0.94$ , quite close to the known exact value  $\beta_c = 1$ . In view of our still shaky line of reasoning concerning the partial compensation of the divergencies plaguing the individual coefficients  $a_4$  and  $a_6$ , this finding is quite encouraging.

Turning at last to the truly interesting case  $d = 2$ , and proceeding as above, we obtain the estimates  $\beta_c^{(4)}$  and  $\beta_c^{(6)}$  listed in Table 1; a linear fit of these data over  $1/\nu_m$  then provides the limit  $\beta_c = 0.7029$  for  $\nu_m \rightarrow \infty$ . Similarly, we compute finite-order estimates  $\zeta^{(\nu_m)}$  of the superfluid-density exponent  $\zeta$ , with an imposed twist of either  $\theta/\ell = 0.01$ , or  $\theta/\ell = 0.001$ . First the extrapolation to  $\nu_m = \infty$  is done separately for each twist, as is also documented in Table 1; then a further linear extrapolation to  $\theta/\ell = 0$  gives the final value  $\zeta = 0.6681$ .

### 5 Discussion and outlook

The concept of the effective potential  $\Gamma$ , borrowed from field theory [1, 3], provides an immediate connection between quantum critical phenomena and Landau’s theory of phase transitions [14, 15]. Knowledge of the coefficient  $a_2$  appearing in the Landau expansion (14) of  $\Gamma$  allows one to locate the phase boundary; knowledge of the higher coefficients in the vicinity of that boundary enables one to also monitor the emergence of the order parameter  $|\psi_0|$ , and hence to determine the associated critical exponent  $\beta$ . In Sect. 4 we have applied this scheme to the Mott

**Table 2** Comparison of the critical exponents  $\beta = \beta_c/2$  and  $\zeta$  obtained in this work for the 2D Bose–Hubbard model with data computed by Campostrini et al. [6] for the 3D XY universality class

	This work	Ref. [6]
$\beta$	0.3515	0.3485(2)
$\zeta$	0.6681	0.67155(27)

In the case of  $\zeta$  the relation  $\zeta = \nu$  is utilized

insulator-to-superfluid transition shown by the Bose–Hubbard model, after having computed the Landau coefficients by high-order perturbation theory. In principle, the condensate density then is given by the familiar relation

$$\varrho_c = |\psi_0|^2 = -\frac{a_2}{2a_4} \quad (39)$$

for hopping strengths  $J/U$  slightly above the critical value, so that it should suffice to calculate  $a_2$  and  $a_4$  only. However, our perturbative approximants to these coefficients suffer from the divergency of the weak-coupling perturbation series, so that the above Eq. (39) can be exploited only if our approach is supplemented by a controlled procedure for converting a divergent weak-coupling series into a convergent strong-coupling expansion, as exemplified in Ref. [35]. While such a procedure would require some a priori information on the behavior of the true  $a_4$ , here we have followed a different route, relying on the observation that the divergent behavior of the  $a_4$  approximants is counteracted by that of the approximants to  $a_6$ , as seen in Figs. 5 and 6. Therefore, we keep the sixth-order term in the Landau expansion (31) and replace Eq. (39) for  $\varrho_c$  by its extended analog (17); the same approximation to  $\Gamma$  is employed when evaluating Eq. (26) for the superfluid density  $\varrho_s$ . The critical exponent  $\beta = \beta_c/2$  for the order parameter and the exponent  $\zeta$  for the superfluid density determined in this manner for the 2D Bose–Hubbard model are juxtaposed in Table 2 to the corresponding best known estimates computed for the 3D XY universality class [6]. In the case of  $\zeta$ , we have employed the hyperscaling relation  $\zeta = (d-2)\nu$ , which reduces to  $\zeta = \nu$  for  $d = 3$  and thus equates  $\zeta$  with the critical exponent  $\nu$  for the correlation length [16, 17]. While the accuracy of our results is difficult to specify, and certainly does not match that achieved in Ref. [6], the very fact that the numerical values coincide to better than 1 % constitutes an impressive manifestation of universality.

Yet, our findings still have to be regarded as preliminary. Subsequent steps to be taken now should involve a more systematic processing of the perturbative data, combined with an improved fitting procedure and a reliable error estimate, and it will be important to answer the question whether the encouraging first results reported here can be made more precise [19].

Still, physics is not about producing numbers, but about providing insight. It is, therefore, quite striking to observe that the elemental 2D Bose–Hubbard model actually provides the critical exponents of the lambda transition, and it might be interesting to pin down the “carrier” of this universality in terms of the process-chain diagrams involved in the computation of the Landau coefficients. Is there, perhaps, some simple properties of these diagrams which clarify why the 2D model differs so significantly from the 3D one?

Of course, the ultimate test of universality will also require an experimental high-precision measurement of the critical exponents of the 2D Bose–Hubbard model, as realized with ultracold atoms in planar optical lattices. Besides the experiments referred to in the “Introduction” section, recent studies aiming at the single-site addressability of ultracold atoms in optical lattices [38–41] hold a particularly high promise in this respect, since such techniques may allow one to directly measure spatial correlation functions, and thereby to determine the exponents  $\nu$  and  $\eta$ . In any case, with ultracold atoms now entering the field of critical phenomena, far-reaching further developments lie ahead.

**Acknowledgments** This work was supported by the Deutsche Forschungsgemeinschaft (DFG) under grant No. HO 1771/5. Computer resources have been provided by the HERO cluster of the Universität Oldenburg. A. Pelster gratefully acknowledges a fellowship from the Hanse-Wissenschaftskolleg.

## References

1. J. Zinn-Justin, Quantum field theory and critical phenomena, 4th edn. (Oxford University Press, Oxford, 2002)
2. J.J. Binney, N.J. Dowrick, A.J. Fisher, M.E.J. Newman, The theory of critical phenomena. (Oxford University Press, Oxford, 1992)
3. H. Kleinert, V. Schulte-Frohlinde, Critical properties of  $\Phi^4$  theories (World Scientific, Singapore, 2001)
4. J.A. Lipa, J.A. Nissen, D.A. Stricker, D.R. Swanson, T.C.P. Chui, Phys. Rev. B **68**, 174518 (2003)
5. H. Kleinert, Phys. Lett. A **277**, 205 (2000)
6. M. Campostrini, M. Hasenbusch, A. Pelissetto, P. Rossi, E. Vicari, Phys. Rev. B **63**, 214503 (2001)
7. S. Sachdev, Quantum phase transitions, 2nd edn. (Cambridge University Press, Cambridge, 2011)
8. M.P.A. Fisher, P.B. Weichman, G. Grinstein, D.S. Fisher, Phys. Rev. B **40**, 546 (1989)
9. M. Köhl, H. Moritz, T. Stöferle, C. Schori, T. Esslinger, J. Low Temp. Phys. **138**, 635 (2005)
10. I.B. Spielman, W.D. Phillips, J.V. Porto, Phys. Rev. Lett. **98**, 080404 (2007)
11. I.B. Spielman, W.D. Phillips, J.V. Porto, Phys. Rev. Lett. **100**, 120402 (2008)
12. T. Donner, S. Ritter, T. Bourdel, A. Öttl, M. Köhl, T. Esslinger, Science **315**, 1556 (2007)
13. A. Rançon, N. Dupuis, Phys. Rev. B **84**, 174513 (2011)
14. F.E.A. dos Santos, A. Pelster, Phys. Rev. A **79**, 013614 (2009)

15. B. Bradlyn, F.E.A. dos Santos, A. Pelster, *Phys. Rev. A* **79**, 013615 (2009)
16. M.E. Fisher, M.N. Barber, D. Jasnow, *Phys. Rev. A* **8**, 1111 (1973)
17. J. Rudnick, D. Jasnow, *Phys. Rev. B* **16**, 2032 (1977)
18. A. Eckardt, *Phys. Rev. B* **79**, 195131 (2009)
19. D. Hinrichs, M. Holthaus, A. Pelster, in preparation (2013)
20. R. Feynman, *Phys. Rev.* **56**, 340 (1939)
21. D.D. Fitts, *Principles of quantum mechanics as applied to chemistry and chemical physics.* (Cambridge University Press, Cambridge, 1999), pp. 96–97
22. V.I. Arnold, *Mathematical methods of classical mechanics*, 2nd edn. (Springer, New York, 1989), pp. 61–65
23. A.J. Leggett, *Rev. Mod. Phys.* **71**, S318 (1999)
24. B.S. Shastry, B. Sutherland, *Phys. Rev. Lett.* **65**, 243 (1990)
25. R. Roth, K. Burnett, *Phys. Rev. A* **67**, 031602(R) (2003)
26. T. Kato, *Prog. Theor. Phys.* **4**, 514 (1949)
27. A. Messiah, *Quantum mechanics: volume II.* (Elsevier, Amsterdam, 1999), pp. 712–721
28. N. Teichmann, D. Hinrichs, M. Holthaus, A. Eckardt, *Phys. Rev. B* **79**, 224515 (2009)
29. N. Teichmann, D. Hinrichs, M. Holthaus, A. Eckardt, *Phys. Rev. B* **79**, 100503(R) (2009)
30. N. Teichmann, D. Hinrichs, *Eur. Phys. J. B* **71**, 219 (2009)
31. N. Teichmann, D. Hinrichs, M. Holthaus, *EPL* **91**, 10004 (2010)
32. C. Heil, von der W. Linden, *J. Phys.: Condens. Matter* **24**, 295601 (2012)
33. E. Kalinowski, W. Gluza, *Phys. Rev. B* **85**, 045105 (2012)
34. B. Capogrosso-Sansone, Ş.G. Söyler, N. Prokof'ev, B. Svistunov, *Phys. Rev. A* **77**, 015602 (2008)
35. W. Janke, H. Kleinert, *Phys. Rev. Lett.* **75**, 2787 (1995)
36. B. Capogrosso-Sansone, N.V. Prokof'ev, B.V. Svistunov, *Phys. Rev. B* **75**, 134302 (2007)
37. B.D. Josephson, *Phys. Lett.* **21**, 608 (1966)
38. P. Würtz, T. Langen, T. Gericke, A. Koglbauer, H. Ott, *Phys. Rev. Lett.* **103**, 080404 (2009)
39. N. Gemelke, X. Zhang, C.-L. Hung, C. Chin, *Nature* **460**, 995 (2009)
40. W.S. Bakr, A. Peng, M.E. Tai, R. Ma, J. Simon, J.I. Gillen, S. Fölling, L. Pollet, M. Greiner, *Science* **329**, 547 (2010)
41. J.F. Sherson, C. Weitenberg, M. Endres, M. Cheneau, I. Bloch, S. Kuhr, *Nature* **467**, 68 (2010)